Using Polarization Analyzed SANS To Investigate Magnetic Nanoparticles

1. Introduction

Magnetic nanoparticles and nanoscale structures are intriguing in part because of the exotic properties that can emerge compared with bulk. A reduction of net magnetic moment per atom in magnetite (Fe_3O_4) with decreasing nanoparticle size, for example, is known to occur. This decrease in magnetism has been hypothesized to originate from surface disordering or anisotropy-induced radial canting [1-9], resulting in proposed morphologies that are difficult to verify using conventional magnetometry. Yet, other experiments [10-12] suggest that in certain circumstances oleic acid coating may preserve the surface magnetism. When the nanoparticles are brought close together, additional dipolar interactions come into play.

Application of Polarization Analyzed Small-Angle Neutron Scattering (PASANS) to 9 nm magnetite nanoparticles closed-packed into face-centered crystallites of up to a micron revealed that at nominal saturation the missing magnetic moments unexpectedly interacted to form ordered shells 1.0 to 1.5 nm thick with a magnetic component canted perpendicular to their ferromagnetic cores between 160 to 320 K [13]. These shells additionally displayed intra-particle "cross-talk", *i.e.* they selected a common orientation over clusters of tens of nanoparticles (averaging to zero across the entire sample). However, the shells disappeared when the external field was removed and inter-particle magnetic interactions were negligible (at 300 K), confirming their magnetic origin.

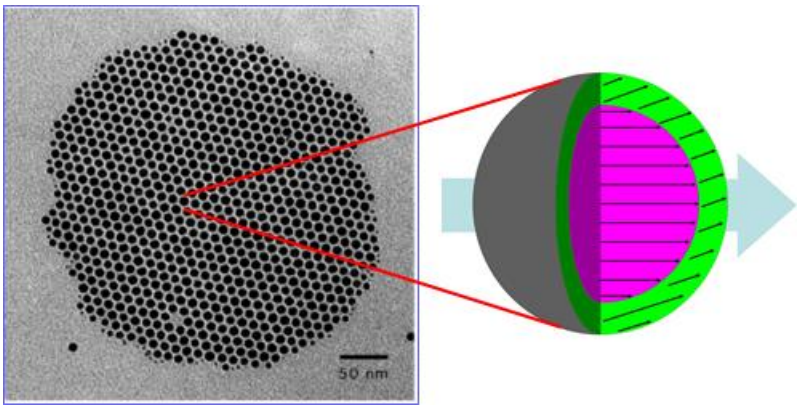

Figure 1 depicts a simplified schematic showing the uniformly canted magnetic shell (green area) with a component that is perpendicular to the applied field of 1.2 Tesla (shown as a light blue arrow).

The canted shell formation is thought to result from the fact that the nanoparticles' crystalline axes are randomly oriented and fixed in place with oleic acid with respect to the applied magnetic field. Each nanoparticle has a preference to magnetically align along its own [111] crystalline axis, denoted magnetocrystalline anisotropy. When a magnetic field is applied, however, it tends to pull the magnetic spins away from this preferred crystalline axis. Since the bonds that hold the magnetic spins in place to are weaker (have fewer nearest neighbor spins to interact with) close to the nanoparticle surface, the spins are more easily canted here in response to the competition between magnetic field determined Zeeman energy and the preferred magnetocrystalline anisotropy direction.

In order to better understand the role of magnetocrystalline anisotropy, we shall study a similar system of close packed 10 nm spherical particles of similar magnetism per volume, but composed of cobalt ferrite ($CoFe_2O_4$) with has a 16 to 18 times higher internal magnetocrystalline anisotropy than Fe_3O_4. Using PASANS we will be able to:

1) Unambiguously separate the structural scattering from the magnetic scattering
2) Separate the magnetic scattering into components that are "parallel to" and "perpendicular to" an external applied field
3) Map how the magnetic canting angle and magnitude varies as a function of field and/or temperature

2. Why Use SANS?

Small-angle x-ray scattering (SAXS) and small-angle neutron scattering (SANS) provide similar information regarding the macroscopic measurement of scattering cross-section, $d\Sigma / d\Omega(q)$. Yet, neutron scattering distinguishes itself in several ways: 1) strong hydrogen scattering cross-section, 2) sensitivity to hydrogen-deuterium substitution, 3) ability to contrast match many samples to solution based on hydrogen-deuterium content, and 4) inherent sensitivity to magnetism. The former properties make neutrons ideal for study of many biological and polymer systems; the latter makes neutrons ideal for studying magnetic systems. Additionally, the manner in which the neutron spin processes upon scattering (to be discussed) allows both the magnitude and *orientation* of sample's magnetic moments to be precisely determined.

3. The SANS Instruments

The NCNR has multiple SANS instruments, but only two of which contain the built in front neutron spin polarizers and spin flippers typically used for full-polarization analysis: Neutron Guide 7 (NG7) SANS and Very Small Angle Neutron Scattering (VSANS). NG7 SANS houses a single, 2D detector which operates by positioning the detector at different distances from the sample and stitching together the data collected at these different configurations. It optimized to cover a q-range of 0.008 nm^{-1} to 7.0 nm^{-1} (0.04 nm^{-1} to 1.3 nm^{-1} in full polarization mode), the former which translates to features sizes below 1 nm and up to 500 nm. Recall that q (sometimes denoted Q) = $2\pi \sin(\alpha) / \lambda \approx 2\pi/\text{distance}$, where α is the scattering angle on the detector with respect to the non-scattered neutron beam center. The VSANS instrument, by contrast, consists of overlapping and translatable sets of detectors which can cover a q-range of 0.002 nm^{-1} to 10 nm^{-1} (or 0.003 nm^{-1} to 1.3 nm^{-1} in full polarization mode) when the high resolution, rear CCD camera is utilized. The maximum q-range with full polarization may be increased in the future with the use of larger ^3He cells. On both instruments, the neutron wavelength (λ) may be tuned between 0.55 nm and 2 nm with a wavelength spread between 11% and 22% full-width half-maximum.

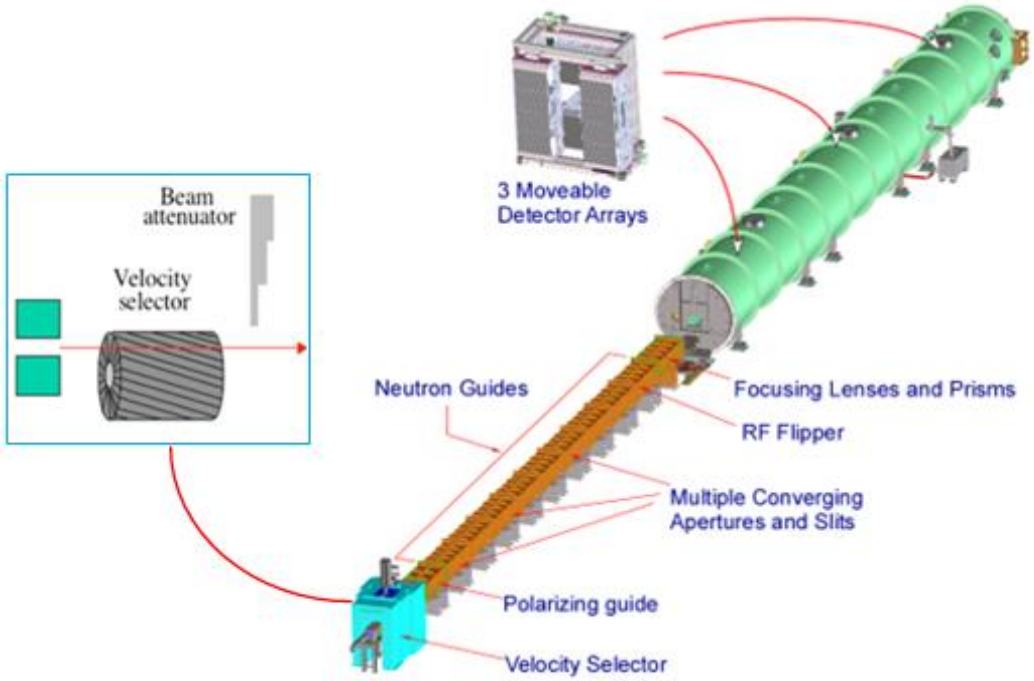

Figure 2 shows a schematic of the VSANS beamline at the NCNR. A traditional SANS beamline is similar, except that it houses a single, two-dimensional detector array which can be translated along the beam path. The sample is located after the neutron guides and before the evacuated detector tank (green).

In the case of a non-polarized (standard) SANS experiment, the intensity of the scattering on the detector after background correction is given by

$$I_{meas} = \phi A d T (\frac{d\Sigma}{d\Omega}) \Delta\Omega \varepsilon t$$

where

ϕ is the number of neutrons per second per unit area incident on the sample

A is the sample area

d is the sample thickness

T is the sample transmission

$\Delta\Omega$ is the solid angle over which scattered neutrons are accepted by the analyzer

ε is the detector efficiency

t is the counting time

The aim of the SANS experiment is to obtain the differential macroscopic scattering cross-section $d\Sigma/d\Omega$ from I_{meas}. During a polarized scattering experiment, the efficiency of the

polarizing components will additionally need to be corrected for (utilizing specialized SANS/VSANS IGOR modules or python-based code), but the fundamental aim remains.

4. Planning the Experiment

4a. Scattering Length Density

In order for there to be small-angle scattering, there must be scattering contrast, in this case between the nanoparticles, oleic acid coating, and air (≈ 0). The scattering is proportional to the scattering length density (abbreviated SLD and symbolized as ρ) *squared*. SLD is defined as

$$\rho = \frac{1}{V}\sum_{i}^{n} b_i$$

where V is the volume containing n atoms, and b_i is the (bound coherent) scattering length of the i^{th} atom in V. V is usually the molecular or molar volume for a homogeneous phase in the system of interest.

Neutrons are scattered either through interaction with the nucleus (nuclear scattering, N) or through interaction between the unpaired electrons (and hence the resultant magnetic moment, M) with the neutron's spin. As example, $CoFe_2O_4$ has both a nuclear SLD and a magnetic SLD and displays both nuclear and magnetic contrast. Nuclear SLDs can be calculated from the above formula, using a table of the scattering lengths [14] for the elements, or calculated using the interactive SLD Calculator available at the NCNR's web pages [15]. Magnetic SLD can be calculated using the following formula

$$\rho_m = M\ \left(in\ \frac{A}{m}\right) x\ 2.853\ x\ 10^{-12}\ \frac{m}{A\ \text{Å}^{-2}}$$

Some handy magnetic conversions are:

$$\frac{A}{M} = \ 1000\,\frac{emu}{cc};\ \ \mu_B = 9.274\ x\ 10^{-21}\ emu$$

The magnetic saturation of *bulk* $CoFe_2O_4$ (at 5 K) is 497.7 emu/cc [16]. Note that nanoparticles may vary from bulk due to dislocations and from the effect of surface termination sites. Table 1 provides some useful SLDs for our experiment.

Material (bulk)	Chemical Formula	SLD_nuclear ($Å^{-2}$)	SLD_magnetic ($Å^{-2}$)
Cobalt ferrite	$CoFe_2O_4$	6.07×10^{-6}	1.42×10^{-6}
Magnetite	Fe_3O_4	6.97×10^{-6}	1.46×10^{-6}
Oleic Acid	$C_{18}H_{34}O_2$	7.81×10^{-8}	0

Table 1. Nuclear and magnetic scattering length densities of interest

4b. Sample Thickness

Given the calculated sample contrast, how thick should the sample be? Recall that the scattered intensity is proportional to the product of the sample thickness, d_s, and the sample transmission, T. It can be shown that the transmission, which is the ratio of the transmitted to the incident beam intensity, is given by

$$T = e^{-\sum_t d_s}$$

where $\sum_t = \sum_c + \sum_i + \sum_a$ (the sum of the coherent, incoherent, and absorption macroscopic cross sections). The absorption cross section, $\sum_a$, can be accurately calculated from tabulated absorption cross sections of the elements (and isotopes) if the mass density and chemical composition of the sample are known. The incoherent cross section, $\sum_i$,can be estimated from the cross-section tables for the elements as well, but not as accurately as it depends on the atomic motions and is, therefore, temperature dependent. The coherent cross section, $\sum_c$, can also only be estimated since it depends on the details of both the structure and the correlated motions of the atoms in the sample. This should be no surprise as $\sum_c$ as a function of angle is the quantity we are aiming to measure!

The scattered intensity is proportional to $d_s T$ and hence

$$I_{meas} \propto d_s e^{-\sum_t d_s}$$

which has a maximum at $d_s = 1/\sum_t$ and implies an optimal transmission at 1/e = 0.37. The sample thickness at which this occurs is known as the "1/e" length.

The NCNR SLD calculator [15] provides estimates of 1/e length, which is about 4.5 mm for $CoFe_2O_4$. However, since our particles are not uniform, but rather have strong repeatable lattice spacing (strong Bragg scattering), we reduce the thickness to avoid multiple scattering. As example, for close-packed ferrite-based nanoparticles, masses in the range of 30 mg to 80 mg have typically worked well.

4c. Selecting Instrument Configurations Using SASCALC / VCALC

SASCALC is a tool built into the SANS IGOR reduction package that allows different beamline configurations to be simulated, helping users to select an ideal balance between desired q-range and maximum beam intensity. One such good configuration for this experiment on NG7 SANS would be:

```
Source Aperture Diameter =      5.00 cm
Source to Sample =               487 cm
Sample Aperture to Detector =    280 cm
Beam diameter =                 4.06 cm
Beamstop diameter =             2.00 inches
Minimum Q-value =             0.0154 1/Å (sigQ/Q = 23.9 %)
Maximum Horizontal Q-value =  0.1456 1/Å
Maximum Vertical Q-value =    0.1456 1/Å
Maximum Q-value =             0.2049 1/Å (sigQ/Q = 4.8 %)
Beam Intensity =           1307589 counts/s
Figure of Merit =             3.27e+07 Å^2/s
Attenuator transmission =     0.00122 = Atten # 8
***************** NG 3 *****************
Sample Aperture Diameter =           0.64 cm
Number of Guides =                   7
Sample Chamber to Detector =         220.0 cm
Sample Position is                   Huber
Detector Offset =                    0.0 cm
Neutron Wavelength =                 5.00 Å
Wavelength Spread, FWHM =            0.109
Sample Aperture to Sample Position =5.00 cm
Lenses are OUT
```

A good configuration for VSANS (using VCALC, http://nicedata.ncnr.nist.gov/niceweb/nicejs/VCALC/) would be:

Beam

λ (Å) 5.5 | Δλ/λ 0.12 | Frontend Trans. = 1.0 | Flux Φ = 1.575e+11 | Beam Current (1/s) = 2.884e+5 | I_0 (1/s/cm^2) = 9.106e+5

Collimation

Num. guides 4 | Source aperture (mm) 60.0 | Source distance (cm) = 1582 | T_filter = 0.5245418835981687 | T_guide = 0.8852928099999999

Ext. Sample aperture (mm) 6.35 | Sample ap. to GV (cm) 75 | Sample to GV (cm) 75

L_1 (cm) = 1507 | A_1A_2/L_1 = 0.000003913

Middle Carriage

SDD input (cm) 1450 | SDD (cm) = 1525 | L_2 (cm) = 1525 | Beam drop (cm) = 0.4384 | Beamstop Required (inch) = 2.976 | Beamstop (inch) 3

$2\theta_{min}$ (rad) = 0.002498 | **Q_{min} (1/A) = 0.002854** | $(\Delta Q/Q_{min})_x$ = 0.4147 | $(\Delta Q/Q_{min})_y$ = 0.4149 | Q_{max} (1/A) = 0.05000 | $(\Delta Q/Q_{max})_x$ = 0.05434 | $(\Delta Q/Q_{max})_y$ = 0.05434

Ref Beam Ctr_x (cm) 0 | Ref Beam Ctr_y (cm) 0 | From file

Left Panel | Lateral Offset (cm) -1.5 | Q_{right} (1/Å) = -0.001854 | **Q_{left} (1/Å) = -0.03142**

Right Panel | Lateral Offset (cm) 0.5 | Q_{left} (1/Å) = 0.0009102 | **Q_{right} (1/Å) = 0.03048** | Q_{bottom} (1/Å) = -0.03901 | Q_{top} (1/Å) = 0.03840

Front Carriage

Q_{min} (1/Å) = 0.03048 | $(\Delta Q/Q_{min})_x$ = 0.06235 | $(\Delta Q/Q_{min})_y$ = 0.06236 | Q_{max} (1/Å) = 0.1881 | $(\Delta Q/Q_{max})_x$ = 0.04939 | $(\Delta Q/Q_{max})_y$ = 0.04939

SDD input (cm) 370 | SDD (cm) = 445 | Ref Beam Ctr_x (cm) 0 | Ref Beam Ctr_y (cm) 0 | From file

Left Panel | Lateral Offset (cm) -11.5176 | Q_{right} (1/Å) = -0.03142 | **Q_{left} (1/Å) = -0.1321** | Match to left edge of ML

Right Panel | Lateral Offset (cm) 11.2799 | Q_{left} (1/Å) = 0.03048 | **Q_{right} (1/Å) = 0.1312** | Match to right edge of MR

Top Panel | Vertical Offset (cm) 15.8467 | Q_{bottom} (1/Å) = 0.03840 | Q_{top} (1/Å) = 0.1306 | Match to top edge of MR

Bottom Panel | Vertical Offset (cm) -15.2487 | Q_{top} (1/Å) = -0.03901 | Q_{bottom} (1/Å) = -0.1312 | Match to bottom edge of MR

5. Magnetic SANS

5a. Magnetic Scattering

Small-angle neutron scattering is ideal for obtaining nuclear and magnetic structure, even for small magnetic moments that aren't necessarily all oriented in the same direction, with sub-nanometer resolution. Normally neutrons are unpolarized, meaning their spins points point randomly in all directions. In the presence of a magnetic field (H), half the neutron spins will align with the field; half anti-parallel to the applied field. The first selection rule of neutron scattering is that only the component of a magnet moment oriented perpendicular to the scattering wave vector, q, participates in scattering. Thus, if an applied magnetic field (H) is set along X and the detector is in the X-Y plane, magnetic moments oriented along Y or Z (M_Y, M_Z) may be detected if measuring along the X-direction, while magnetic moments oriented along X or Z (M_X, M_Z) may be detected if measuring along the Y-direction (Figure 3). Note that an applied magnetic field required to align the neutron spins may be quite small (0.005 Tesla or less).

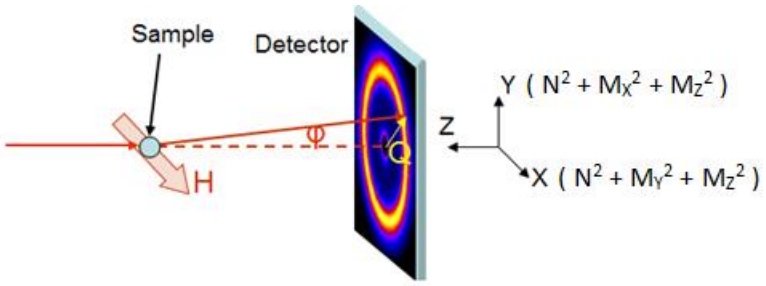

Figure 3. Scattering with an applied magnetic field, H, set along the X-direction. Note how only the components of the sample magnetism perpendicular to q (noted on right hand side) may be seen in the scattered intensity.

Assuming that the nuclear scattering is isotropic, this gives a way to separate nuclear and magnet scattering contributions. The measured scattering intensity, I, is proportional to the squared sum of the spatial nuclear (N^2) and magnetic (M^2) Fourier transforms, defined as

$$N, M_J(q) = \sum_K \rho_{N,M_J}(K) e^{iq \cdot R_K}$$

where J is any Cartesian coordinate, $\rho_{N,M}$ is the nuclear or magnetic scattering length density, and R_K is the relative position of the K^{th} scatterer. Note that because we can only measure the absolute value of the Fourier Transform squared in a scattering experiment, rather than the

complex components of the Fourier Transform itself, we lose *phase* information. The result is that we may not be able to uniquely distinguish between a family of curves that model our data – a fact that should be kept in mind during data fitting and analysis.

Now, let us consider the case of Fe_3O_4 nanoparticles under the influence of a *saturating* magnetic field of 1.2 Tesla, such that the magnetic spins align along X (|| H). In this case, the X-axis contains only nuclear scattering, while the Y-axis contains nuclear scattering plus magnetic scattering from moments along X (M_X^2), as shown in the Figure 4.

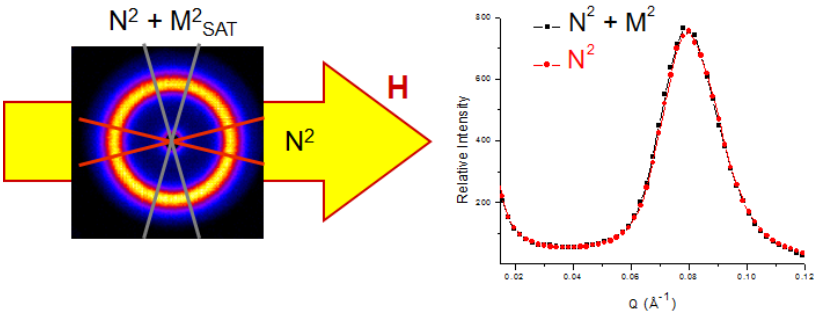

Figure 4. Comparison of horizontal and vertical sector cuts, with H || X, can be used to separate nuclear and magnetic scattering contributions if the structural scattering is isotropic. Scattering from a sample of Fe_3O_4 nanoparticles at 1.2 Tesla is shown.

In Figure 4, the diffraction peak comes from the fact that the nanoparticles are close-packed into μm-sized, ordered , face-centered cubic arrays with a prominent [111] diffraction peak centered at 0.08 $Å^{-2}$. The reason that the sector cuts along X and Y are so similar, although only the latter contains the magnetic scattering contribution, is that the ratio of magnetic to nuclear scattering, ρ^2_M / ρ^2_N is only 4% (refer to Table 1). For this reason, *polarization analyzed* SANS is useful to directly measure the magnetic scattering when the magnetic scattering contribution is small compared to the structural scattering contribution (demonstrated in section 5b. using the same Fe_3O_4 sample).

5b. Polarization Analysis

As discussed previously, an applied magnetic field realigns the spins of a neutron beam, normally randomly oriented, so that half of the spins become parallel with H, and the other half become anti-parallel to H. Now, one spin state can be preferentially selected over the other, using a polarizing element such an FeSi supermirror. The supermirror is a specially made magnetic diffraction grating that looks different to neutrons aligned parallel and anti-parallel to the applied field, thus scattering neutron spins of one orientation (denoted ↓) while allowing the spins of the orientation to pass through (denoted ↑). From here, the ↑ neutrons can be reversed at will using an electromagnetic flipper coil or an radiofrequency flipper. After

interaction with the sample, an analyzing glass cell filled with polarized ^{3}He preferentially allows neutrons with spins aligned with the ^{3}He atoms to pass through, while absorbing neutrons with oppositely aligned spins. This differs from the supermirror in that a divergently scattered beam, not just a tightly collimated one, may be surveyed at once. The ^{3}He orientation can be reversed at will with a nuclear magnetic resonance (NMR) pulse of an appropriate frequency. This combination, depicted in Figure 5, allows one to measure scattering cross-sections of ↑↑, ↓↑, ↓↓, and ↑↓ (where the first arrow indicate the spin before sample scattering and the second arrow indicates the neutron spin after sample scattering). These can also be denoted as Up (U) or Down (D) neutrons, or even as + and – neutrons.

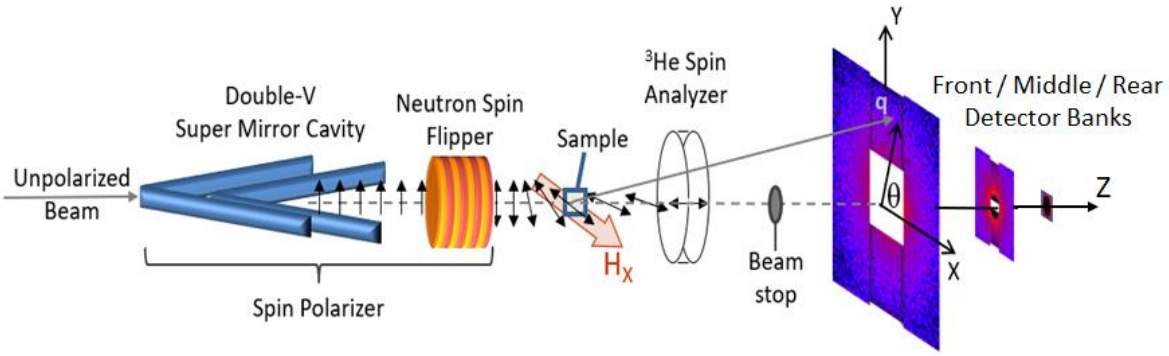

Figure 5. Polarization analysis set-up for a SANS instrument consists of a spin polarizing supermirror, a neutron spin flipper, a sample area with a variable applied magnetic field, a spin analyzing ^{3}He cell, and a 2D detector or detector array (as depicted).

As will be discussed in more detail, the ^{3}He polarization is time dependent. Yet, the polarization efficiency of each polarizing element can be measured with neutrons and corrected for within the SANS reduction framework. For any polarizing/analyzing element, the degree of polarization, P, is defined as the difference between the ↑ and ↓neutrons after passing through a polarizing device, divided by the total number of incoming neutrons (↑ + ↓):

$$P = \frac{\uparrow - \downarrow}{\uparrow + \downarrow}$$

The utility of adding polarization analysis for measuring M^2 is immediately obvious from Figure 6. Sector slices about the X-axis and Y-axis, resulting from the ↑↑ and ↓ ↓ scattering cross-sections, contain easily observable ±NM cross-terms.

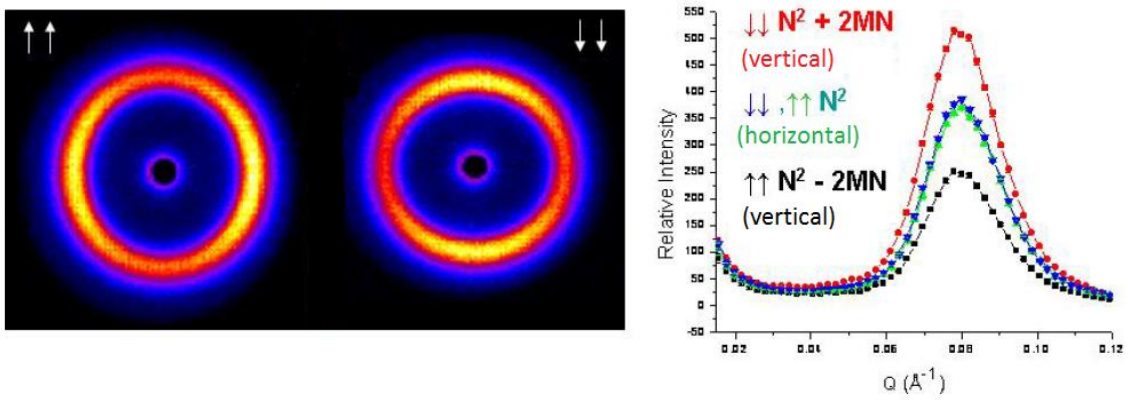

Figure 6. The net magnetism from a magnetically semi-saturated or saturated sample can be more readily observed using polarization analysis than using unpolarized neutrons (see Figure 4) when the nuclear scattering dominates the magnetic scattering. The sample shown consists of Fe_3O_4 nanoparticles in a field of 1.2 Tesla.

5c. Spin Selection Rules

The original rule (discussed for unpolarized neutrons) that only the component of M $\perp$ Q can participate in scattering also holds true for polarized neutrons. Additionally, of this projection of M $\perp$ Q, the part that is also || to the neutron polarization axis (defined by H) does not reverse the neutron spin. The remaining projection of M $\perp$ Q that is $\perp$ to the neutron polarization axis (defined by H) does reverse the neutron spin. These processes are denoted as non spin-flip (NSF) and spin-flip (SF) scattering, respectively. The nuclear scattering does not affect the neutron spin, and so all structural scattering is confined to the NSF scattering. These rules are summarized in Figure 7.

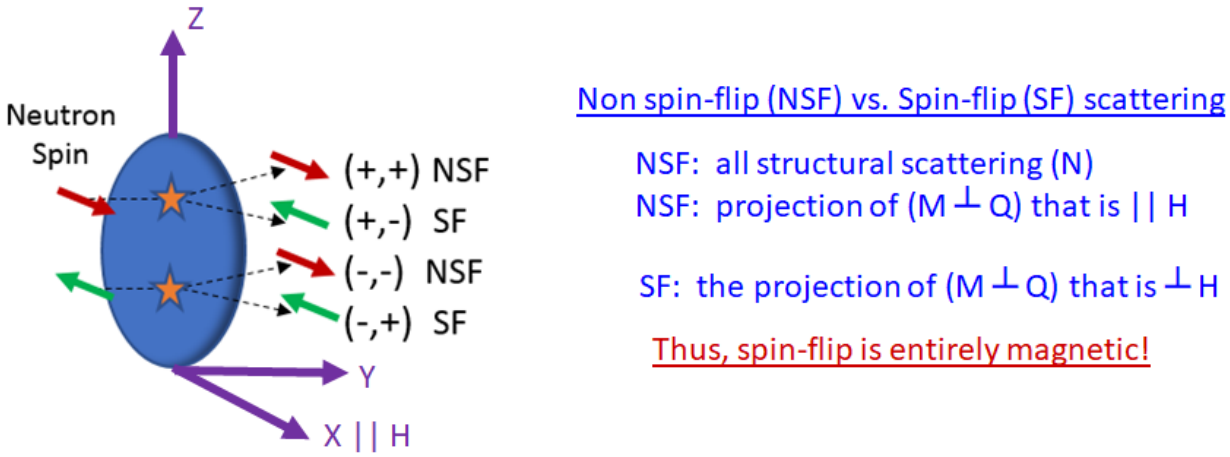

Figure 7. A summary of the nuclear and magnetic spin scattering selection rules. The magnetic field, H, which sets the neutron polarization axis, is shown || X, while the incident neutron beam is || Y.

The spin selection rules can be represented mathematically in terms of the Halpern-Johnson vector [17], which translates into the following equations [18-19] where H || X and θ is the angle between the positive X-axis and Q:

$$I^{\downarrow\downarrow,\uparrow\uparrow} = |N|^2 + sin^4(\theta)|M_X|^2 + \ sin^2(\theta)cos^2(\theta)|M_Y|^2 - [M_X{}^*M_Y + M_Y{}^*M_X]sin^3(\theta)cos^1(\theta) \pm [M_X{}^*N + N^*M_X]sin^2(\theta) \mp [M_Y{}^*N + N^*M_Y]sin^1(\theta)cos^1(\theta)$$

$$I^{\uparrow\downarrow,\downarrow\uparrow} = |M_Z|^2 + cos^4(\theta)|M_Y|^2 + \ sin^2(\theta)cos^2(\theta)|M_X|^2 - [M_X{}^*M_Y + M_Y{}^*M_X]sin^1(\theta)cos^3(\theta) \pm i[M_Z{}^*M_X - M_X{}^*M_Z]sin^1(\theta)cos^1(\theta) \mp i[M_Z{}^*M_Y - M_Y{}^*M_Z]cos^2(\theta)$$

Note that the equations simplify greatly along the X and Y axis. This is shown pictorially in Figure 8 using the Fe_3O_4 example data discussed previously.

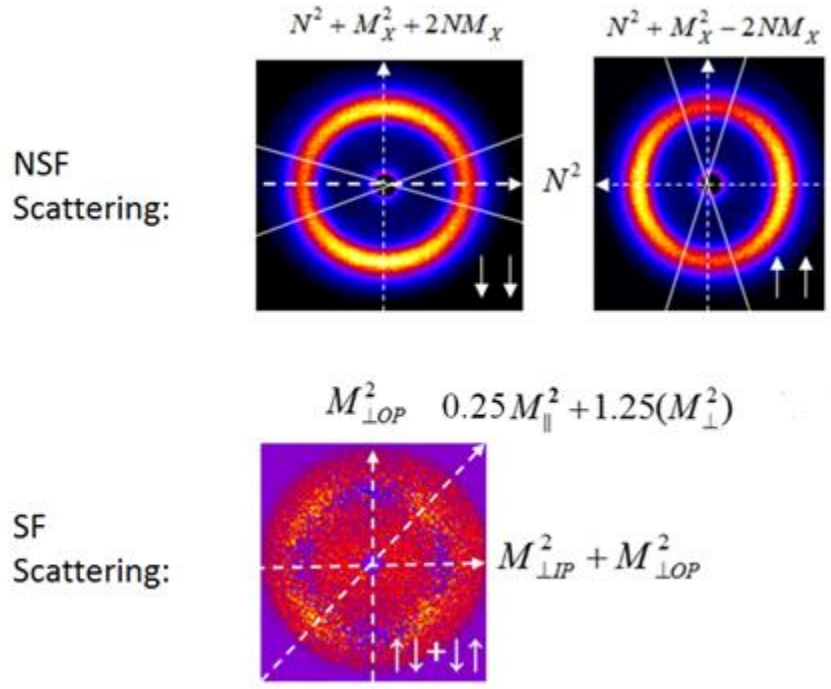

Figure 8. Simplification of the magnetic scattering equations occurs along the coordinate axes, as shown by the white arrows. Note the spin-flip scattering pattern is entirely magnetic, while the non spin-flip scattering contains the nuclear scattering contribution. The sample shown consists of Fe_3O_4 nanoparticles at 1.2 Tesla.

Thus, the following operations can be performed [18] to extract specific components of interest:

$$|N|^2 = I^{\uparrow\uparrow}(\theta = 0^o) = I^{\downarrow\downarrow}(\theta = 0^o)$$

$$|M_X|^2 = [I^{\downarrow\downarrow}(\theta = 90^o) + I^{\uparrow\uparrow}(\theta = 90^o)] - [I^{\downarrow\downarrow}(\theta = 0^o) + I^{\uparrow\uparrow}(\theta = 0^o)], assuming\ \ isotropic\ |N|^2$$

$$|Net\ M_X|^2 = \frac{[I^{\downarrow\downarrow}(\theta = 90^o) - I^{\uparrow\uparrow}(\theta = 90^o)]^2}{8|N|^2}, assuming\ \ isotropic\ |N|^2$$

$$|M_\perp|^2 = \frac{I^{\uparrow\downarrow}(\theta = 0^o) + I^{\downarrow\uparrow}(\theta = 0^o) + I^{\uparrow\downarrow}(\theta = 90^o) + I^{\downarrow\uparrow}(\theta = 90^o)}{3}, assuming\ \ |M_Y|^2 = |M_Z|^2$$

$$|M_X|^2 = 4[I^{\uparrow\downarrow}(\theta = 45^o) + I^{\downarrow\uparrow}(\theta = 45^o)] - 5|M_\perp|^2, assuming\ \ |M_Y|^2 = |M_Z|^2$$

Let us now apply these operations once more to the Fe_3O_4 example system at 200 K in an applied magnetic field of 1.2 Tesla (|| X). The results are shown in Fig. 9 where sector slices of ± 10° are taken about the X and Y axis to approximate θ = 0° and 90° degree scattering respectively. We can now clearly see that the nuclear Bragg peak of height 1000 A.U. in intensity dominates the M^2_X (labeled generically as M^2_{PARL}) Bragg peak of 30 (in directly comparable units). This indicates that the sample is almost saturated, and M^2_X has the same periodic spacing as N^2 (i.e. all nanoparticles within a crystalline lattice have a sizeable magnetic component oriented along X). Additionally, M^2_Y and M^2_Z (labeled generically as M^2_{PERP}) are small, but not negligible. In fact, they can be modeled as a canted shell 1 nm thick [13] with some uniform magnetic component oriented perpendicular to the applied field per particle. This magnetic core-canted shell morphology can be made to disappear by reducing the applied field to 0.005 Tesla at 300 K [13] (not shown).

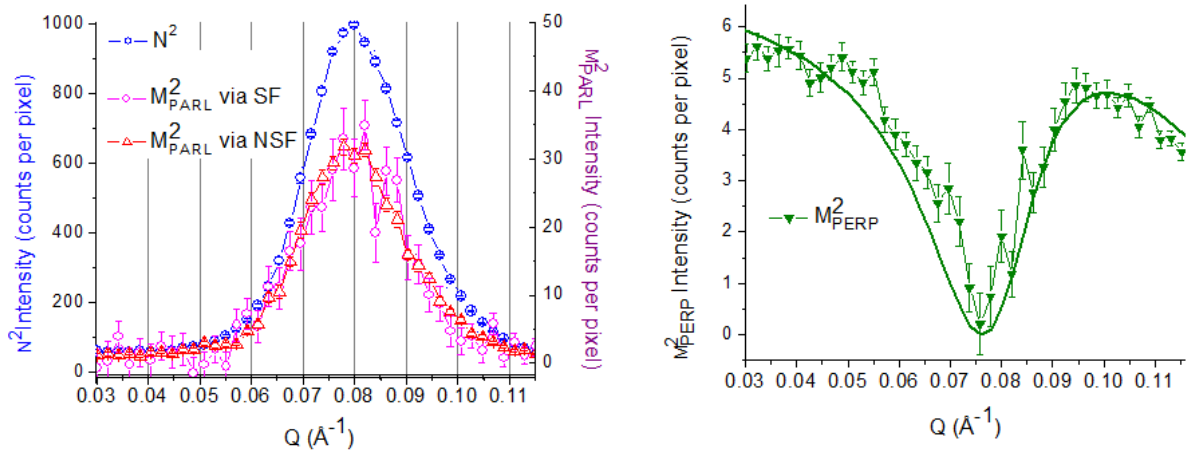

Figure 9. Applying the sector cuts, shown in Figure 8, results in the separation of nuclear scattering, magnetic moments along X || H (M^2_{PARL}), and magnetic moments along Y or Z ⊥ H (M^2_{PERP}). Note there is than one way to extract M^2_{PARL}.

6. Data Collection

Let us return the experiment at hand: $CoFe_2O_4$ close-packed nanoparticles. In order to properly reduce the data, several types of data files were collected. Transmissions are collected with the beam stop removed (translated to the side) in order to survey the unscattered neutron beam; these are taken with a series of attenuating filters to ensure this main neutron beam isn't so intense so as to saturate the detector. Scattering files, on the other hand, make use of a beam stop that blocks this main beam in order to emphasize the weaker sample scattering observed at higher angles. In this case, a sufficiently large beam stop (1" to 4" possible depending on detector distance and beam collimation) is chosen so that no attenuating filters are typically required. Note that initially transmission file(s) will be used to define the beam center (from which Q is calculated), while scattering file(s) will be used to align the beam stop with respect to the main beam. Post-set up, the transmissions are used to normalize the data, while the scattering files contain the desired q-dependent scattering.

6a Instrument Alignment

Your instrument responsible/contact will typically align your configuration(s) that has been chosen with the aid of SASCALC or VCALC (discussed in 4c). For clarity, the alignment steps will be briefly described here. (1) The wavelength and wavelength spread, detector distance(s), number of neutron guides, number of attenuators, source and sample aperture sizes and distances, sample position, and beam stop size are entered, see Figure 10. (2) A transmission measurement is taken by translating the beam stop out of the main beam, often to a fixed position of – 15.0 cm. The X, Y coordinates of the beam center are determined from the intensity-weighted average of the transmission, and these values are entered back into the configuration. (3) On VSANS, these X, Y beam center coordinates can be used to fine tune the front detector panel lateral offsets w.r.t. the middle detectors using VCALC so that complete 2D q-coverage is achieved. (4) Using the sample itself or an intense scattering source such as Teflon, scattering files are collected and the X-beam stop and Y-beam stop coordinates are iteratively adjusted until the beam stop is centered on the main beam. This is done for each configuration. (5) A flat-scatterer such as glassy carbon is often measured in each scattering configuration to define a mask for any areas over which the neutrons can't scatter unimpeded. (6) If the sample can be viewed directly, a silicon mirror located within the neutron guides can be temporarily inserted to deflect a red light down the beam line which illuminates the neutron path while the sample is centered on the beam. If the sample is housed in an opaque container, such as a closed-cycle refrigerator for example, a neutron camera can be used to visualize the sample and its local shielding w.r.t. the main beam. (7) If multiple samples will be measured on a translation stage, the centered position of each may be recorded. (8) Once the sample(s) is

centered, the neutron beam is temporarily blocked with a neutron absorber so that both 'blocked beam' scattering and transmission files are recorded per configuration. This allows one to subtract off dark current and neutron scattering into the detector from nearly beam lines. Now alignment is complete.

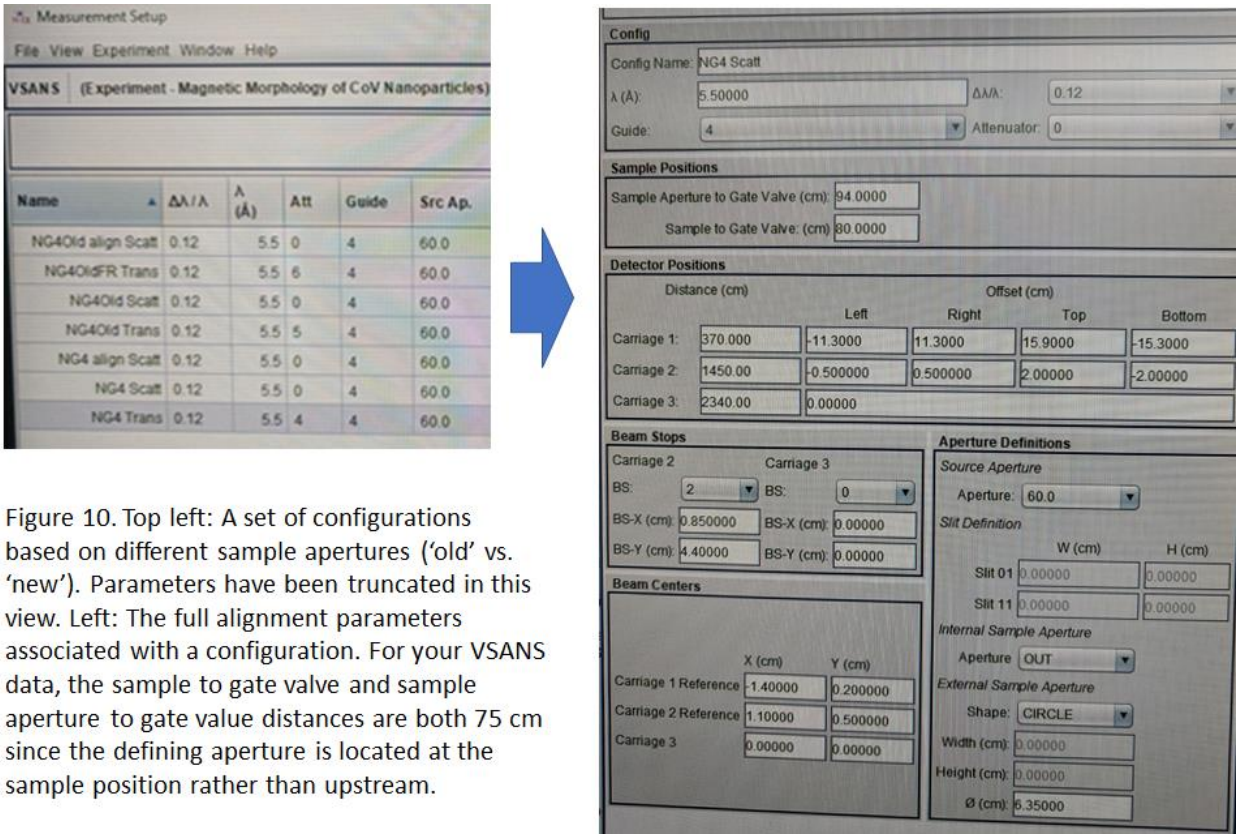

Figure 10. Top left: A set of configurations based on different sample apertures ('old' vs. 'new'). Parameters have been truncated in this view. Left: The full alignment parameters associated with a configuration. For your VSANS data, the sample to gate valve and sample aperture to gate value distances are both 75 cm since the defining aperture is located at the sample position rather than upstream.

6b Normalization of scattering intensity onto an absolute scale

Your data include transmissions (all at the same attenuation and detector distance) from the sample in a sample holder (a sealed Al can), the sample holder by itself, and an open beam (no sample or sample holder). These will provide absolute scale normalization.

6c Unpolarized transmissions through the ^{3}He analyzer

The ^{3}He spin filter (analyzer) is pre-pumped into a polarized state with optical pumping, but decays over time with a half-life on the order of 150 – 250 hours. In order to measure the effective polarization of this filter and the reduction in transmission of the preferred spin state over time, a series of *unpolarized* (*i.e*. supermirror moved out of the beam) transmissions through the ^{3}He filter were measured. Precisely, this includes a series of open beam transmissions (^{3}He translated out of the beam), ^{3}He transmission (^{3}He translated into the

beam), and a blocked beam transmission – all taken for the same counting time (100 seconds), at the same detector distance and with the same number of attenuators. A blocked beam measurement was also collected in order to correctly subtract the stray neutrons that make their way into the detector from neighboring beam lines.

6d Polarized transmissions to correct for supermirror and flipper polarization efficiency

Four polarized transmissions (↑↑, ↓↑, ↓↓, and ↑↓) plus a blocked beam were taken in order to calculate the polarizing efficiency of the super mirror, the spin flipper, and any sample depolarization. Although the ^{3}He transmission is calculated as a function of time, these four transmissions are usually taken back-to-back for the best results.

6e Polarized scattering files

Four (or more) polarized data scattering files (↑↑, ↓↑, ↓↓, and ↑↓) plus four polarized data-holder scattering files (↑↑, ↓↑, ↓↓, and ↑↓) were collected. One of each type of scattering is needed; multiples of any one type can be added together for increased counting statistics. Typically, we break the scattering into multiple chunks of no more than an hour each to provide the best time-dependent correction. The samples scattering files will be corrected for polarizer inefficiencies of the super mirror, spin flipper, and ^{3}He spin analyzer using the transmission measurements noted above. The data-holder scattering files (also called empty scattering files) are similarly corrected for polarizing optics inefficiencies, and they are subtracted from the sample within its sample holder scattering to remove background. All this is taken care of within the SANS IGOR or python-based framework, the conceptual details of which are explained in [19].

6f. Acquiring the necessary files

At both NG7 SANS and VSANS, we can utilize the polarized beam module shown in Table II. At the top the sample name is set, as well as the thickness and intent. Note that intent can be sample, open, empty, or blocked beam. In general, you will want to take scattering and transmission blocked beam measurements near the beginning of an experiment per instrument configuration so as to be able to subtract our dark noise and stray neutrons. Blocked beams measurements are especially important for making sure the front and middle detectors match in intensity. In the body of Table II, the left columns are used to set the states of interest (polarization type, number of scattering files, temperature, magnetic field, and selected detector configuration(s) as defined in section 6a), while the three, right-most columns are used to run the associated transmission or scattering files. The column labeled '3He' takes the measurements needed to calculate the ^{3}He polarization (*i.e.* transmissions with the ^{3}He cell translated out of and then into the neutron beam), and this is ideally measured every four to six hours or so (the sample can remain in place if desired). The 'Trans' column takes the

transmissions needed for proper scaling and characterization of the sample + instrument depolarization (*i.e.* transmissions of UU, DU, DD, UD, and super mirror only with ^{3}He translated out of the beam for full-polarization, U and D transmissions for half polarization, and a non-polarized transmission if unpolarized is selected), and it should be performed at least once per unique sample + temperature + magnetic field condition. Finally, the Scatt column will automatically run the number of polarized, half-polarized, or unpolarized scattering files listed to the left for the time specified. For full polarization measurements, it is imperative to take at least one of UU, DU, DD, and UD scattering measurement per sample + temperature + magnetic field condition in order to be able to fully polarization correct your data. The exception to this is a sample (or empty) where it is known that no magnetic scattering is present – then one non spin-flip (UU or DD) plus one spin-flip (DU or UD) scattering files will suffice. As long as the sample name is consistent and the intent is properly labeled, we have a python program available that will automatically associate the correct transmission and scattering files together for an "automatic" reduction.

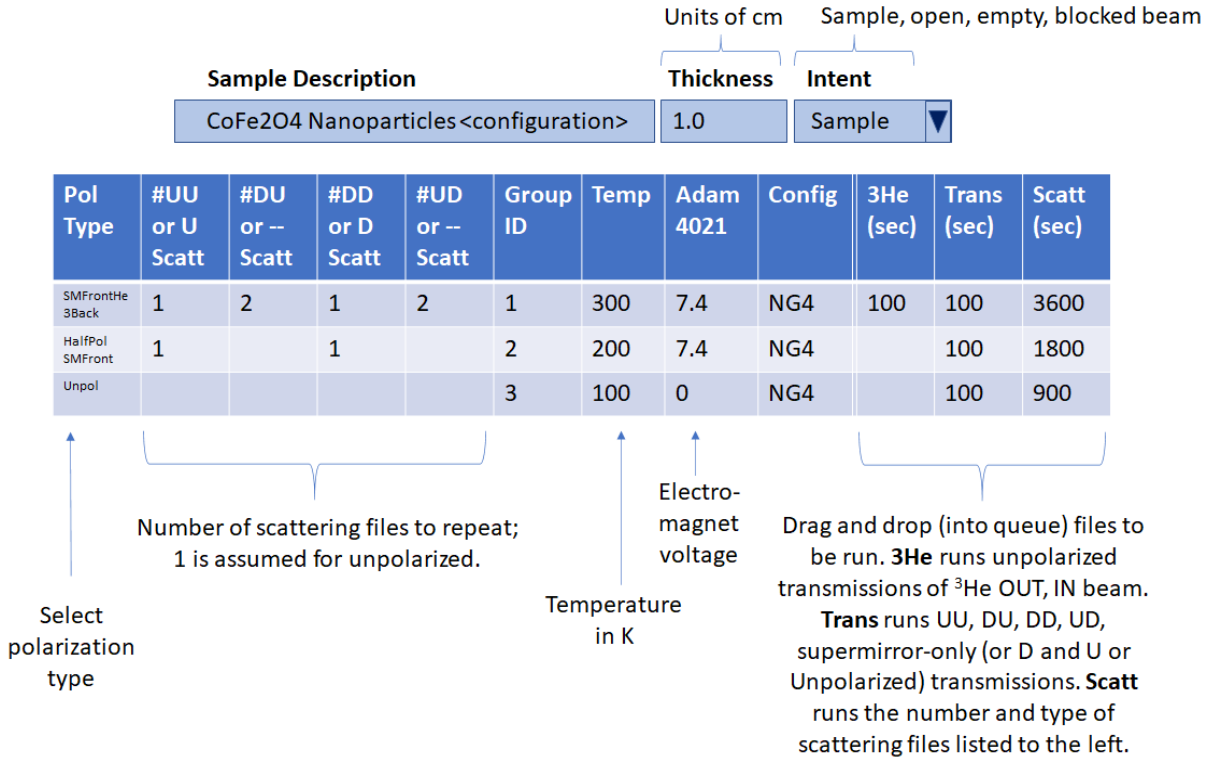

Pol Type	#UU or U Scatt	#DU or -- Scatt	#DD or D Scatt	#UD or -- Scatt	Group ID	Temp	Adam 4021	Config	3He (sec)	Trans (sec)	Scatt (sec)
SMFrontHe 3Back	1	2	1	2	1	300	7.4	NG4	100	100	3600
HalfPol SMFront	1		1		2	200	7.4	NG4		100	1800
Unpol					3	100	0	NG4		100	900

Table II. Polarization module in the NICE data acquisition interface. Selecting and dragging boxes from the three right-most columns create the measurements necessary to measure the time-dependent ^{3}He polarization (labeled 3He), to measure the scaling factor as well as the sample + beam line depolarization (labeled Trans), or to run the specified scattering cross-sections for the number of times listed in order to collect sufficient statistics (labeled Scatt).

7 Data Viewing

Live (current) data can be viewed at https://www.ncnr.nist.gov/ipeek/. A VSANS example is shown in Figure 10, where small a gap between the middle (center) and front (outer) detector panels can be seen. It is often best to eliminate this gap for magnetic samples where the scattering is anisotropic and horizontal vs. vertical sector cuts are often compared, rather than circularly averaged.

Additionally, all the recorded instrumental parameters related to the data files taken can be found on https://ncnr.nist.gov/ncnrdata/view/nexus-hdf-viewer.html?pathlist=ncnrdata. Data files can be downloaded, 10 at a time, from this site. However, to download larger data sets we recommend a python script that will be distributed in the class.

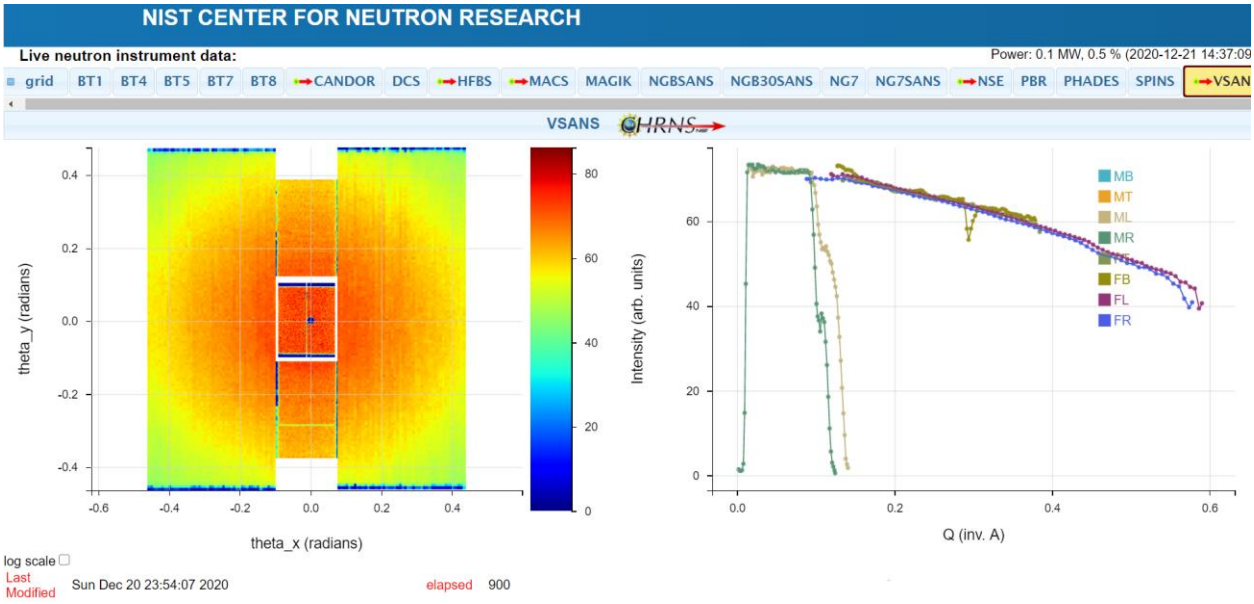

Figure 11. An example of live data taken at VSANS. On the right, M and F refer to middle and front detector banks, respectively. B, T, L, and R refer to bottom, top, left, and right, respectively,

8 Data Reduction

You will be using a combination of data collected on close-packed $CoFe_2O_4$ nanoparticles taken at NG7 SANS and VSANS using full polarized neutron beam. The former measurements involve a series of temperatures, while the latter surveys a more crystalline sample across a range of magnetic fields at 300 K. Both samples were made by the Majetich group at Carnegie Mellon University.

The reduction will be performed using a python-based script in class (the same principles are followed in the IGOR-based polarized SANS reduction, except that the grouping of data requires

less manual intervention in the python version). The first step involves identifying all the ^{3}He transmissions, along with an appropriate blocked beam measurement, in order to construct a time-dependent decay curve per ^{3}He cell used during the experiment. From here on, the timestamp on all other ^{3}He polarized measurements can be used to calculate the time-dependent transmission of the majority and minority neutron spins traversing through the ^{3}He cell. The second step involves grouping the polarized transmissions per sample + temperature + applied magnetic field condition, and from these plus an appropriate blocked beam measurement, the polarization of the sample and beam line depolarization will be determined. Finally, the scattering files per sample + temperature + applied magnetic field condition will also be grouped and associated with the appropriate polarization parameters determined in the second step. The leakage due to sample depolarization and polarizing elements that are less than 100% efficient will be corrected for such that properly scaled and pure UU, DU, DD, and UD scattering cross-sections will be obtained. If empty polarized transmission and scattering files exists, these can be subtracted off after proper polarization correction and scaling by transmission. As long as the data are all properly labeled, these steps will be automatically performed for each sample condition. Our job is to check the resulting output to make sure all the generated values and data files make sense, correcting incorrectly labeled files or excluding bad ones (such as ones where the beam shutter was not opened, etc.). The final scattering data can be viewed as 2D images with the detector overlap appropriately masked or in the form of 1D circular averages or sector cuts.

9 Data Analysis

Using the angular cuts discussed in Section 5, you will transform your reduced scattering data (Section 8) into nuclear and magnetic scattering contributions. Fortunately, we have built some of the most commonly used manipulations into the python code in order to directly generate these for you. You will have several choices to make regarding sector cut width and whether to treat your sample as structurally isotropic or not. From here, The SANS IGOR Analysis package [20], and its successor SASView [22], will be used to model these scattering profiles, including factors such as smearing from wavelength spread, collimation, and sample polydispersity. In particular, you will be heavily using the core-shell model, face-centered cubic (FCC) paracrystal model, and the body-centered cubic (BCC) paracrystal model. More information about these models can be found at [23]. Your instructors will work with you to model your data and extract key information regarding the nuclear (structural) and magnetic morphology.

Specifically, you should be able to answer the following questions regarding the 10 nm $CoFe_2O_4$ close-packed nanoparticle system:

- What is the average spacing between the nanoparticles?

- How much of the sample magnetization has a component that does not lie along the applied magnetic field at high and low applied magnetic fields?
- What is the magnetic to nuclear intensity ratio at high field (> 1 Tesla)? How does this compare with bulk $CoFe_2O_4$?
- What form factor best fits the $M \perp H$ component: a core-shell model like the one observed for the Fe_3O_4 nanoparticles, a model in which the surface spins are disordered, or something else?
- Can the measured morphology be understood in terms of a competition between Zeeman and magnetocrystalline anisotropy energies?
- Do the two samples differ in terms of magnetic responsiveness?

10 References

[1] P. Dutta et al., J. Appl. Phys. 105, 07B501 (2009)

[2] J. Curiale et al., Appl. Phys. Lett. 95, 043106 (2009)

[3] A. Kovacs et al., Phys. Rev. Lett. 103, 115703 (2009)

[4] C. Westman et al., J. Phys. D 41, 225003 (2008)

[5] R. Yanes et al., Phys. Rev. B 76, 064416 (2007)

[6] J. Mazo-Zuluaga, J. Restrepo, and J. Maria-López, Physica (Amsterdam) 398B, 187 (2007)

[7] J. Mazo-Zuluaga et al., J. Appl. Phys. 105, 123907 (2009)

[8] L. Berger et al., Phys. Rev. B 77, 104431 (2008)

[9] Y. Hu A and Du, J. Nanosci. Nanotechnol. 9, 5829 (2009)

[10] J. Salafrana et al., Nano Lett 12, 2499-2503 (2012)

[11] M. Darbundi et al., J. Phys. D: Appl. Phys. 45, 195001 (2012)

[12] A. G. Roca et al., J. Appl. Phys. 105, 114309 (2009)

[13] K.L. Krycka et al., Phys. Rev. Lett. 104, 207203 (2010)

[14] V.F. Sears, Neutron News 3, 29-37 (1992)

[15] http://sld-calculator.appspot.com/

[16] S.R. Ahmed et al., Appl. Phys. Lett. 80, 1616 (2002)

[17] R.M. Moon, T. Riste, and W.C. Koehler, Phys. Rev. 181, 920 (1969)

[18] A. Michels and J. Weissmuller, Rep. Prog. Phys. 71, 066501 (2008)

[19] K.L. Krycka et al., J. Appl. Cryst. 45, 554 (2012)

[20] http://www.ncnr.nist.gov/programs/sans/data/red_anal.html, S.R. Kline, J Appl. Cryst. 39, 895 (2006)

[21] K.L. Krycka et al., J. Appl. Cryst. 45, 546 (2012)

[22] https://www.sasview.org/

[23] ftp://ftp.ncnr.nist.gov/pub/sans/kline/Download/SANS_Model_Docs_v4.10.pdf